Published in final edited form as:
*Neuron*. 2011 March 10; 69(5): 957–973. doi:10.1016/j.neuron.2011.02.004.

# Requirement for Plk2 in orchestrated Ras and Rap signaling, homeostatic structural plasticity, and memory

**Kea Joo Lee**[1], **Yeunkum Lee**[1], **Aaron Rozeboom**[1], **Ji-Yun Lee**[1], **Noriko Udagawa**[1], **Hyang-Sook Hoe**[2], and **Daniel T.S. Pak**[1,*]

[1] Department of Pharmacology, Georgetown University Medical Center, 3900 Reservoir Road NW, Washington, DC 20057-1464, USA

[2] Department of Neurology, Georgetown University Medical Center, 3900 Reservoir Road NW, Washington, DC 20057-1464, USA

## Summary

Ras and Rap small GTPases are important for synaptic plasticity and memory. However, their roles in homeostatic plasticity are unknown. Here, we report that polo-like kinase 2 (Plk2), a homeostatic suppressor of overexcitation, governs the activity of Ras and Rap via coordination of their regulatory proteins. Plk2 directs elimination of Ras activator RasGRF1 and Rap inhibitor SPAR via phosphorylation-dependent ubiquitin-proteasome degradation. Conversely, Plk2 phosphorylation stimulates Ras inhibitor SynGAP and Rap activator PDZGEF1. These Ras/Rap regulators perform complementary functions to downregulate dendritic spines and AMPA receptors following elevated activity, and their collective regulation by Plk2 profoundly stimulates Rap and suppresses Ras. Furthermore, perturbation of Plk2 disrupts Ras and Rap signaling, prevents homeostatic shrinkage and loss of dendritic spines, and impairs proper memory formation. Our study demonstrates a critical role of Plk2 in the synchronized tuning of Ras and Rap, and underscores the functional importance of this regulation in homeostatic synaptic plasticity.

## INTRODUCTION

Homeostatic synaptic plasticity is proposed to restrain neuronal firing within appropriate operating limits despite prolonged fluctuations in network activity (Turrigiano, 2008). Attractive candidates underlying adaptive responses to synaptic overexcitation include activity responsive genes that exert negative feedback control over synaptic activity or excitability (Shepherd and Huganir, 2007). Polo-like kinase 2 (Plk2; also called SNK), an activity-inducible member of the polo-like family of serine/threonine kinases, is highly upregulated in central neurons by strong synaptic stimulation (Kauselmann et al., 1999). Plk2 triggers degradation of the dendritic spine-enriched protein SPAR via phosphorylation-dependent ubiquitination (Pak and Sheng, 2003), leading to loss of mature spines and excitatory synapses (Pak and Sheng, 2003; Seeburg et al., 2008). Furthermore, Plk2 is required for homeostatic adaptation in response to elevated or epileptiform activity (Seeburg and Sheng, 2008). Thus, Plk2 exerts physiological and morphological downregulation of

[*]Corresponding author: Daniel T.S. Pak, Ph.D., Department of Pharmacology, Georgetown University Medical Center, 3900 Reservoir road NW, Washington, DC, 20007, Tel: 202-687-8750, Fax: 202-687-8825, dtp6@georgetown.edu.

excitatory synapses following heightened activity, at least in part by depletion of SPAR, a negative regulator of Rap small GTPases (Pak et al., 2001).

Rap and Ras are closely related molecular switches occupying central but often opposing roles in synaptic plasticity (Ye and Carew, 2010). Ras promotes long-term potentiation (LTP) and surface delivery of AMPA receptors (AMPARs), whereas Rap mediates long-term depression (LTD) or depotentiation and AMPAR internalization (Zhu et al., 2002; Zhu et al., 2005). Ras also stimulates overproduction of dendritic protrusions or spines (Arendt et al., 2004; Wu et al., 2001), while Rap promotes spine loss (Fu et al., 2007; Pak et al., 2001; Ryu et al., 2008). Numerous synaptic regulators of Ras/Rap have been identified, including activators (guanine nucleotide exchange factors (GEFs) that stimulate exchange of bound GDP for GTP) and inactivators (GTPase activating proteins (GAPs) that accelerate intrinsic GTPase activity to hydrolyze bound GTP to GDP). The Rap GAP SPAR and the Ras GAP SynGAP both interact with the scaffold protein PSD-95 in the postsynaptic density (PSD) (Chen et al., 1998; Kim et al., 1998; Pak et al., 2001). SPAR promotes spine growth (Pak et al., 2001), while SynGAP deficiency hyperactivates the Ras effector ERK, increases AMPAR surface clusters, and enlarges dendritic spines (Kim et al., 2003; Komiyama et al., 2002; Vazquez et al., 2004), supporting the idea that Ras drives spine growth in opposition to Rap.

Additionally, the Ras GEF RasGRF1/CDC25Mm interacts with NMDA receptor (NMDAR) subunit GluN2B and is required for memory consolidation (Brambilla et al., 1997) and NMDA-dependent ERK activation (Krapivinsky et al., 2003). PDZGEF1 (or RapGEF2/nRapGEP/CNrasGEF/RA-GEF), a neural-specific activator for both mammalian Rap proteins Rap1 and Rap2 (de Rooij et al., 1999; Liao et al., 1999), associates with synaptic scaffolding protein S-SCAM (Ohtsuka et al., 1999), but PDZGEF1 function at synapses is unclear.

Here, we report that Plk2 phosphorylates a quartet of Ras and Rap regulators: SynGAP, PDZGEF1, RasGRF1 and SPAR, resulting in powerful bidirectional control over Rap and Ras activity. These GEFs and GAPs cooperate to downregulate excitatory synapses, dendritic spines, and surface AMPARs following chronic overexcitation. Furthermore, perturbation of Plk2 function disrupts Ras and Rap signaling cascades, abolishes overactivity-dependent synaptic remodeling, and impairs memory formation. These findings show that coordinated regulation of Ras and Rap by Plk2 is critical for homeostatic plasticity and memory.

## RESULTS

To identify novel Plk2 substrates, we tested a panel of synaptic proteins for modification by cotransfected Plk2 in COS-7 cells. Candidates included PSD-95, SAP97, Chapsyn-110, GKAP, AMPAR subunits GluA1/A2, NMDAR subunits GluN1/N2B, Shank, CRIPT, CASK, α-actinin, liprin α1, Epac, Epac2, and Repac, but none of these candidates were reproducibly affected by Plk2 (Fig. S1A, B; data not shown). The only proteins strongly modified were RasGRF1, SynGAP, PDZGEF1, and SPAR (Fig. 1A–D and Fig S1C). With SynGAP and PDZGEF1, Plk2 caused pronounced SDS-PAGE gel mobility shifts without changes in total expression, suggestive of phosphorylation (Fig. 1A, B). Indeed, constitutively active (CA) Plk2 mutant T236E (Ma et al., 2003b) caused greater gel shift than did wild-type (WT) Plk2 (Fig. 1A), while Plk2 kinase-dead (KD) mutant K108M had no effect on SynGAP or any of the candidates (Fig. 1A–D). Treatment of immunoprecipitated SynGAP with calf intestinal alkaline phosphatase abolished its gel shift (Fig. S1D), confirming phosphorylation of SynGAP.

Plk2 contains an N-terminal kinase domain and conserved C-terminal polo box domain (PBD) that mediates substrate recognition and subcellular targeting (Lee et al., 1998). As expected, neither the kinase domain nor PBD alone affected SynGAP migration, suggesting that efficient phosphorylation of SynGAP requires PBD-mediated substrate recruitment (Fig. 1A). In contrast to SynGAP and PDZGEF1, Plk2 dramatically reduced steady-state protein levels of RasGRF1 and SPAR in a dose-dependent manner, consistent with target degradation (Fig. 1C, D and Fig. S1C). Loss of RasGRF1 in presence of CA Plk2 could be largely blocked by proteasome inhibitor MG132 (Fig. 1C), similar to Plk2-mediated degradation of SPAR (Pak and Sheng, 2003). Furthermore, KD Plk2 competitively inhibited WT Plk2 from degrading SPAR in a dominant negative manner (Fig. S1E).

To demonstrate direct phosphorylation by Plk2, we immunoprecipitated RasGRF1, SynGAP, PDZGEF1, or SPAR singly expressed in COS-7 cells (Fig. 1E) for *in vitro* kinase reactions. Immunoprecipitates were incubated with $^{32}$P-γ-ATP and bacterially purified CA or KD Plk2 fused to glutathione-S-transferase (GST). CA Plk2, but not KD Plk2, robustly phosphorylated each of these Ras/Rap regulators in this defined system, while negative controls liprin α1 and GFP were unaffected (Fig. 1F). Thus, the identified Ras/Rap GEFs and GAPs were all direct Plk2 substrates.

In addition, as previously shown for SPAR (Pak and Sheng, 2003), endogenous RasGRF1, SynGAP, and PDZGEF1 from mouse brain lysates were each coimmunoprecipitated by rabbit anti-Plk2 antibody, but not by IgG (Fig. 1G), indicating Plk2 associated with the identified GEFs/GAPs of Ras and Rap *in vivo*. Plk2 could also be coimmunoprecipitated with each regulator when cotransfected in COS-7 cells (Fig. 1H–J), again similar to Plk2 interaction with SPAR (Pak and Sheng, 2003).

## Plk2 is required for overactivity-dependent loss of RasGRF1 and SPAR

To investigate the functional significance of Plk2 phosphorylation of GEFs/GAPs, we confirmed that each Ras/Rap regulator was found in a punctate distribution at excitatory synapses, colocalized with PSD-95 and apposed to the presynaptic marker synaptophysin (Fig. S2A–D; data not shown). To determine if Plk2 induction could degrade endogenous RasGRF1, we treated cultured hippocampal neurons with picrotoxin (PTX, 100 μM, 24 h), a $GABA_A$ receptor antagonist that potently induces Plk2 protein expression (Pak and Sheng, 2003)(also see Fig. S4B, C). PTX-treated neurons exhibited profound loss of both RasGRF1 and SPAR immunoreactivities (Fig. 2A–C) (19±3% of RasGRF1 and 37±5% of SPAR compared to vehicle) in proximal dendrites where Plk2 is enriched (Pak and Sheng, 2003), but not in distal dendrites (Fig. 2A–C). Transfection of Plk2 also decreased fluorescent intensity of RasGRF1 (38±6%) and SPAR (23±6%) to a similar degree as PTX treatment (Fig. 2D–F). These results demonstrated that elevated Plk2 was sufficient to deplete RasGRF1 and SPAR in specific dendritic regions of hippocampal neurons.

To test if Plk2 was required for overactivity-dependent degradation of RasGRF1 and SPAR, we employed three independent methods to inhibit Plk2 function: 1) KD Plk2, a dominant-negative inhibitor of WT Plk2 (Fig. S1E); 2) BI2536, a potent and selective inhibitor of Plk family kinases (Plks 1–4) (Lenart et al., 2007); and 3) RNA interference (RNAi) to specifically and effectively silence Plk2 expression (Fig. S4A–D). As above, PTX caused extensive loss of RasGRF1 and SPAR in proximal dendrites relative to basal control, along with more modest decreases in PSD-95: GFP-expressing neurons (RasGRF1, 23±5%; SPAR, 26±7%; PSD-95, 40±4%) (Fig. 2G, H); no BI2536 (RasGRF1, 21±3%; SPAR, 27±4%; PSD-95, 32±5%) (Fig. 2I, J); and transfected with empty pLL3.7 vector (RasGRF1, 23±7%; SPAR, 13±3%; PSD-95, 34±5%) (Fig. 2K, L). For PSD-95, puncta number was highly correlated with integrated intensity values (Fig. S2E-G), suggesting decreases in PSD size as well as number, supported also by immunofluorescent intensity and puncta density

for another postsynaptic marker, Shank (Fig. S2H–J). Because Plk2 did not affect PSD-95 expression in COS-7 cells (Fig. S1A), the dismantling of PSD scaffold proteins in neurons was likely indirect.

In contrast, blocking Plk2 function or expression fully abolished these responses to PTX: expression of KD Plk2 (RasGRF1, 109±28%; SPAR, 102±15%; PSD-95, 90±8%; $p>0.41$) (Fig. 2G, H); treatment with BI2536 (75 nM, 20 h) (RasGRF1, 86±6%; SPAR, 105±13%; PSD-95, 108±24%; $p>0.29$) (Fig. 2I, J); and knockdown of Plk2 (RasGRF1, 154±26%; SPAR, 128±14%; PSD-95, 134±5%; $p>0.38$) (Fig. 2K, L). To control for RNAi off-target effects, we coexpressed Plk2-shRNA with a shRNA-resistant rescue construct of Plk2 (Fig. S4A, E) and observed significantly reduced fluorescent intensity or puncta number of RasGRF1, SPAR, and PSD-95 (Fig. S4E–G), similar to the effect of WT Plk2 overexpression alone. Interestingly, knockdown of the highly related polo-like kinase Plk3 with a specific shRNA construct (Fig. S4H–K) had no effect on PTX-mediated loss of synaptic proteins (Fig. S4L, M), suggesting a specific role for Plk2 in this process.

Although expression of KD Plk2 (Fig. 2D–F) or knockdown of Plk2 for 3 days in the absence of PTX caused a significant overaccumulation in RasGRF1, SPAR, PSD-95, and Shank levels (Fig. 2F, L and Fig. S2I–J) (KD Plk2: RasGRF1, 148±24%; SPAR, 165±15%; Shank, 150±14%; Plk2 RNAi: RasGRF1, 169±24%; SPAR, 147±16%; PSD-95, 139±11%; $p<0.05$), BI2536 treatment alone for 20 h did not (Fig. 2J and Fig. S2F) (RasGRF1, 102±14%; SPAR, 110±14%; PSD-95, 111±13%; $p>0.52$), likely due to the shorter length of time of Plk2 inhibition.

Moreover, PTX effects were occluded in neurons expressing WT Plk2 (RasGRF1, 20±4%; SPAR, 24±3%; PSD-95, 33±5%; $p<0.001$ for each vs GFP and $p>0.28$ vs GFP+PTX) (Fig. 2G, H and Fig. S2E), indicating that Plk2 and PTX operate by overlapping mechanisms. Collectively, these data demonstrated a specific requirement for Plk2 in homeostatic removal of RasGRF1, SPAR, and excitatory synaptic scaffolding following chronic overactivity.

## Plk2 promotes SynGAP and PDZGEF1 activity

Because Plk2 phosphorylated SynGAP and PDZGEF1 without reducing their expression, we examined their enzymatic activity against Ras and Rap. We used GST linked to the Ras binding domain (RBD) of the Ras effector Raf1 as an affinity reagent that specifically pulls down active Ras (de Rooij and Bos, 1997)(Fig. S3A). With this assay we found that SynGAP modestly reduced activity of cotransfected WT H-Ras, as expected (Fig. 3A, B) (Kim et al., 1998). Levels of active Ras were further diminished when SynGAP and Ras were cotransfected with Plk2 (Fig. 3A, B). Plk2 by itself had no effect on Ras, indicating that Plk2 exerted regulation of Ras via SynGAP (mean density: Ras, 0.48±0.03; Ras +SynGAP, 0.35±0.03, $p<0.05$; Ras+SynGAP+Plk2, 0.21±0.02, $p<0.001$ vs Ras alone and $p<0.05$ vs Ras+SynGAP; Ras+Plk2, 0.54±0.09, $p=0.58$).

Similarly, active Rap pulldown assays were carried out using GST fused to the Rap binding domain of RalGDS, a downstream effector of Rap (Zwartkruis et al., 1998), that bound only to active Rap (Fig. S3B). When WT Rap2 was transfected alone, only a small amount of active Rap2 was observed (Fig. 3C). Cotransfection of PDZGEF1 significantly stimulated Rap2 activity, consistent with Rap GEF function (de Rooij et al., 1999). Levels of active Rap2 were further boosted when Plk2 was cotransfected with PDZGEF1 and Rap2 (Fig. 3C, D). Plk2 by itself did not affect active Rap2 levels, suggesting that Plk2 activated Rap by enhancing the GEF activity of PDZGEF1 (mean density: Rap2, 0.15±0.06; Rap2+PDZGEF1, 0.59±0.11, $p<0.01$; Rap2+PDZGEF1+Plk2, 1.15±0.11, $p<0.001$ vs Rap2

alone and p<0.01 vs Rap2+PDZGEF1; Rap2+Plk2, 0.26±0.09, p=0.36). Thus, Plk2 was sufficient to promote the activities of both SynGAP and PDZGEF1 in mammalian cells.

### Plk2 is required for overactivity-dependent regulation of Ras and Rap

To directly test effects of Plk2 on Ras and Rap in neurons, we infected hippocampal neurons with Sindbis virus expressing EGFP, WT Plk2, or KD Plk2 for 24 h, and then performed active Ras and Rap pulldown assays. Remarkably, neurons expressing WT Plk2 showed nearly a complete absence of active H-Ras, along with much higher levels of active Rap2 compared to cultures expressing GFP or KD Plk2 (Fig. 3E, F), resulting in ~110-fold change in the relative activity of Rap vs Ras (Fig. 3G; p<0.05) (active Ras: GFP, 0.28±0.03; WT Plk2, 0.02±0.01, p<0.001; KD Plk2, 0.33±0.08, p=0.61; active Rap2: GFP, 0.09±0.02; WT Plk2, 0.68±0.11, p<0.01; KD Plk2, 0.11±0.01, p=0.29). Plk2 overexpression also markedly reduced activation of the downstream Ras target ERK and increased active p38 (a Rap target) compared to GFP-expressing or untransfected neurons (Fig. S3C–F). Conversely, KD Plk2 expression significantly increased phospho-ERK (Fig. S3D), but did not affect phospho-p38 (Fig. S3F).

Induction of endogenous Plk2 by PTX treatment of neurons also decreased active Ras levels while elevating levels of active Rap (Fig. 3H, I) (~8.6-fold increase in relative Rap vs Ras activity; Fig. 3J; p<0.01) (active Ras: control, 0.47±0.03; PTX, 0.16±0.03, p<0.01; BI2536+PTX, 0.49±0.05, p=0.83; active Rap2: control, 0.14±0.02; PTX, 0.40±0.02, p<0.001; BI2536+PTX, 0.15±0.01, p=0.67). These PTX-mediated effects were blocked by coincubation with Plk inhibitor BI2536 (Fig. 3H–J), suggesting that native Plk2 directs overactivity-dependent bidirectional shifts in Ras and Rap signaling.

### Plk2 is required for overactivity-dependent spine remodeling

Plk2 induction promotes elimination of mature dendritic spines (Pak and Sheng, 2003). To examine if loss of Plk2 affected spine morphology, we transfected neurons with Plk2-shRNA. Plk2 knockdown for 3 days significantly increased spine density and spine head size in proximal dendrites compared to control (Fig. 4A, C) and also blocked PTX-induced decreases in spine density and head area (Fig. 4B, D; quantified in F, G, and Table S1). Coexpression of the Plk2 rescue construct suppressed the Plk2-shRNA phenotypes and further decreased spine density and head size below control values (Fig. 4E–G). Moreover, acute disruption of Plk2 function using BI2536 also prevented PTX-dependent reduction in spine density and head width (Fig. 4H–M; Table S1). However, we did not observe increased spine number or head size in neurons treated with BI2536 by itself for 20 h, again possibly reflecting the difference between acute and chronic disruption of Plk2 function. No significant differences were detected in spine length under any conditions (Table S1). We also did not observe changes in spine density and morphology in distal dendrites of PTX-treated neurons (Fig. S4N–Q), consistent with our immunostaining results (Fig. 2A–C). These data demonstrated that Plk2 is critical for homeostatic downregulation of proximal dendritic spines following overactivity.

### Ras and Rap regulators are essential for Plk2-induced spine remodeling

To determine the roles and relative importance of individual Ras/Rap regulators in Plk2-directed spine plasticity, we first transfected hippocampal neurons with GFP-expressing shRNA constructs generated against each regulator (Fig. S5F; knockdown efficiency shown in Fig. S5A–E). Quantitative analysis of proximal dendritic spines showed distinct effects for each regulator. RasGRF1 knockdown significantly reduced spine density and length compared to control vector, while silencing of SPAR reduced head width and spine density (Fig. S5G–I; Table S1). Loss of SynGAP greatly increased spine head size with no change in other parameters, and PDZGEF1 RNAi increased only spine density (Fig. S5G–I; Table

S1). These changes in spine head size and number were highly correlated with the results of immunofluorescent intensity and puncta density for PSD-95 (data not shown). Moreover, coexpression of shRNA-resistant rescue constructs completely prevented the spine phenotypes observed with silencing their cognate Ras/Rap regulators (Fig. S5F–I; Table S1), demonstrating RNAi specificity. Thus, the Ras/Rap regulatory proteins govern overlapping but non-identical aspects of dendritic spines (Fig. S5J).

Because Plk2 degraded RasGRF1/SPAR, while stimulating SynGAP/PDZGEF1, we reasoned that overexpression of RasGRF1/SPAR, or silencing of SynGAP/PDZGEF1, may block Plk2-induced reduction in spine density and head width (Fig. 5A, B, G and H). Indeed, coexpression of either RasGRF1 or SPAR with Plk2 increased spine density and head size compared to Plk2 alone (Fig. 5C, F–H; Table S1). Knockdown of SynGAP in the presence of Plk2 markedly increased spine head width (Fig. 5D and H) with no change in spine density (Fig. 5G), while silencing of PDZGEF1 with Plk2 expression increased spine number without change in spine head size (Fig. 5E, G and H; Table S1). Thus, reduction of RasGRF1/SPAR and enhancement of SynGAP/PDZGEF1 all contribute to Plk2 effects on spines (Fig. 5I).

We further tested whether modulation of Ras/Rap regulation could rescue the increased spine density and head width caused by Plk2 RNAi (Fig. 5J, K, P, Q; Table S1). Knockdown of Plk2 increases RasGRF1/SPAR levels, and is predicted to decrease SynGAP/PDZGEF1 activity; therefore, silencing of RasGRF1/SPAR or overexpression of SynGAP/PDZGEF1 may be expected to reverse the effects of Plk2 RNAi. Silencing of RasGRF1 and Plk2 together reduced spine density to control level, although spine head width remained similar to Plk2 knockdown alone (Fig. 5L, P, Q; Table S1). Knockdown of SPAR and Plk2 together showed a significant decrease in both spine density and head width (Fig. 5O–Q). Cotransfection of SynGAP with Plk2-shRNA markedly decreased spine head size without change in spine density (Fig. 5M, P, Q), whereas coexpression of PDZGEF1 with Plk2-shRNA reduced spine density without change in head width (Fig. 5N, P, Q). No significant differences were observed in spine length in any condition (Table S1). Collectively, these data demonstrate that Ras/Rap GEFs and GAPs act downstream of Plk2, and further support the idea that different regulators control specific aspects of spine morphology and density (Fig. 5I, R).

## Plk2 phosphorylation of Ras/Rap regulators is required for overactivity-dependent spine remodeling

To determine the requirement for Plk2 phosphorylation of Ras/Rap regulators in spine morphogenesis, we identified Plk2-dependent phosphorylation sites in target substrates using tandem mass spectrometry. In total, we detected 6 novel sites for RasGRF1, 8 sites for SynGAP, and 5 sites for PDZGEF1 that were specifically phosphorylated in the presence of active Plk2 (Fig. S6A).

We next tested if RasGRF1 phosphorylation was required for its degradation by Plk2. COS-7 cells were transfected with WT or phosphomutants of RasGRF1 and either KD or CA Plk2. As before, WT RasGRF1 levels were greatly diminished by active Plk2 (Fig. S6B). However, mutation of either serine 71 or 575 to alanine (S71A or S575A) substantially abolished loss of RasGRF1 by Plk2 (Fig. S6B). Intriguingly, both mutants reside within RasGRF1 pleckstrin homology (PH) domains, motifs that mediate membrane association (Buchsbaum et al., 1996). Indeed, the phosphomutants displayed higher enrichment in membrane fractions (Fig. S6C), suggesting that Plk2 phosphorylation of RasGRF1 PH domains causes membrane dissociation as a prelude to degradation.

For SynGAP, either of two phosphomutants (S781A or S783A) largely blocked the gel mobility shift induced by Plk2 (Fig. S6D), implying a critical role of these adjacent phosphosites for conformational changes in SynGAP. Active Ras pulldown assays demonstrated that these sites, as well as S326 and S390, were also crucial for Plk2 to stimulate SynGAP activity against Ras (Fig. S6E, F; Table S2).

In the case of PDZGEF1, we observed no differences in Plk2-dependent gel mobility shift or alterations in Rap GEF activity with any single Plk2 phosphosite mutant (Fig. S6G). Various double, triple, and quadruple phosphomutant combinations of PDZGEF1 also yielded no effect on mobility shift or GEF activity (data not shown). However, loss of all 5 Plk2 phosphosites (5×A mutant) substantially blocked the mobility shift of PDZGEF1 by Plk2 (Fig. S6G, right panel) and the Plk2-mediated increase in enzymatic activity of PDZGEF1 towards Rap (Fig. S6H, I; Table S2).

Next, to evaluate the functional importance of these phosphosites for overactivity-dependent spine remodeling, we performed quantitative spine analysis in proximal dendrites of neurons expressing the most severe mutants of RasGRF1 (S71A), SynGAP (S390A or S783A), and PDZGEF1 (5×A) (Fig. 6A). Transfection of either WT or RasGRF1 (S71A) increased spine density compared to GFP control (Fig. 6B–D, J; Table S1). PTX application significantly reduced spine density in neurons expressing WT RasGRF1, but this effect was partially blocked in neurons expressing RasGRF1 (S71A) (Fig. 6C, D, J). WT RasGRF1 also increased spine head size, which was reversed in the presence of PTX (Fig. 6K). In contrast, PTX treatment failed to reduce spine head width in neurons expressing RasGRF1 (S71A) (Fig. 6K).

Expression of WT or phosphomutants of SynGAP strongly reduced spine head size (Fig. 6E–G, L; Table S1) without changing spine density. PTX treatment of neurons expressing WT SynGAP led to even further reduction of head width as well as spine loss (perhaps due to some spine sizes falling below the cutoff threshold for detection) (Fig. 6E, J, L). In contrast, these PTX effects were abolished in neurons expressing either SynGAP phosphomutant (Fig. 6F, G, J, L).

Lastly, either WT or PDZGEF1 (5×A) mutant decreased spine density without changing head size (Fig. 6H–J, M; Table S1). PTX treatment further decreased spine density in neurons expressing WT PDZGEF1, but not in neurons expressing the quintuple phosphomutant (Fig. 6H–J). However, neither WT nor PDZGEF1 (5×A) mutant affected PTX-dependent reduction of spine head size (Fig. 6M). There was no significant difference in spine length in any condition (Table S1). Together, these results suggested that phosphorylation of Ras/Rap regulators by Plk2 is required for homeostatic regulation of dendritic spines following chronic overactivity.

### Plk2 phosphorylation of Ras/Rap regulators controls surface AMPARs

We recently showed that Plk2 promotes loss of surface GluA2 (sGluA2) via an atypical kinase-independent mechanism in distal dendrites (Evers et al., 2010). To elucidate the role of Plk2 phosphorylation in AMPAR surface expression, we stimulated neuronal activity while blocking Plk2 kinase activity (with BI2536) or Plk2 expression (with Plk2-RNAi). PTX treatment markedly decreased surface GluA1 (sGluA1) expression only in proximal dendrites, with no change in distal dendrites, and this decrease was abolished by either BI2536 or Plk2 RNAi (Fig. 7A, C). In contrast, PTX reduced sGluA2 in both proximal and distal dendrites (Fig. 7B, D), consistent with previous findings (Evers et al., 2010). Interestingly, coincubation of BI2536 with PTX rescued sGluA2 expression only in proximal dendrites, but not distal dendrites, while Plk2 RNAi increased basal sGluA2 expression in both proximal and distal dendrites and abolished PTX-induced removal of

sGluA2 in either region (Fig. 7B, D). No changes in total GluA1/A2 were observed under any conditions (data not shown and Evers et al., 2010). Thus, sGluA1/A2 on proximal dendrites were regulated by a Plk2 kinase-dependent mechanism, whereas the kinase-independent mechanism specifically affected sGluA2 in distal dendrites.

We next examined the role of Ras/Rap regulators in overactivity-induced reduction of AMPARs. Cultured neurons were transfected with shRNA against RasGRF1 or SPAR in the absence of synaptic stimulation to test if inactivation of Ras or activation of Rap is sufficient to cause loss of surface AMPARs. As expected, knockdown of SPAR reduced sGluA1/A2 expression in proximal dendrites (Fig. 7E–H). Silencing of RasGRF1 also decreased sGluA1 but only showed a nonsignificant trend for sGluA2 removal (Fig. 7E–H, $p=0.10$). We then transfected neurons with shRNA constructs for SynGAP or PDZGEF1 and stimulated with PTX to induce endogenous Plk2. PTX-mediated loss of sGluA1/A2 was completely abolished by silencing SynGAP or PDZGEF1 (Fig. 7E–H). These results demonstrate that tuning down of Ras or tuning up of Rap is necessary and sufficient for PTX-induced reduction of AMPARs in proximal dendrites.

Finally, we investigated whether Plk2 phosphorylation of Ras/Rap regulators is important for the PTX effects on surface AMPARs. As before, PTX stimulation reduced sGluA1/A2 levels in proximal dendrites (Fig. 7I–L). Overexpression of RasGRF1 WT or its phosphomutant (S71A) significantly increased sGluA1 expression, and the sGluA1 loss by PTX was partially blocked in neurons expressing S71A (Fig. 7I, K). In contrast, RasGRF1 expression did not increase sGluA2 levels or prevent PTX-mediated removal of sGluA2 (Fig. 7J, L), confirming the above result that silencing of RasGRF1 did not greatly reduce sGluA2 (Fig. 7G, H). Expression of SynGAP WT or PDZGEF1 WT reduced sGluA1/A2 and there was further reduction of sGluA1/A2 after PTX stimulation (Fig. 7I–L). Phosphomutants of SynGAP (S783A) and PDZGEF1 (5×A) similarly reduced sGluA1/A2 levels but blocked the additional loss of surface AMPARs by PTX. Thus, Plk2 phosphorylation of these Ras/Rap regulators is required for PTX-induced downregulation of surface AMPARs in proximal dendrites.

## Disrupted Ras and Rap signaling in DN-Plk2 mice

To study the role of Plk2 *in vivo*, we generated transgenic (TG) mice that express dominant negative (DN) kinase-dead Plk2 in the postnatal forebrain (Fig. 8A) via the CaMKIIα promoter (Mayford et al., 1996). After identifying DN-Plk2 lines by PCR genotyping (Fig. 8B), in situ hybridization revealed transgene mRNA specifically in the adult DN-Plk2 forebrain, in a pattern similar to the endogenous Plk2 mRNA (Fig. 8C). Native Plk2 protein was weakly detectable by immunohistochemistry in WT mice, while high levels of Plk2 (likely DN-Plk2) were observed in TG hippocampus and cortex (Fig. 8D). Western blot analysis showed that expression of DN-Plk2 was ~250% of endogenous Plk2 in TG mice (Fig. 8E; $p<0.05$). The expression pattern of transgene suggested DN-Plk2 may effectively compete with and inhibit native Plk2, as it does in heterologous cells and neurons (Fig. S1E and Fig. 2F).

Immunoblotting of forebrain lysates showed no differences in total expression of several synaptic proteins between genotypes (Fig. S7A). However, DN-Plk2 mice expressed higher levels of RasGRF1 and SPAR compared to WT animals (Fig. 8H, I), suggesting an imbalance between Ras and Rap in TG mice. Pulldown assays to measure active Ras, Rap1 and Rap2 showed that DN-Plk2 mice contained greater Ras activity than WT littermates, and most remarkably, nearly a complete absence of active Rap1 or Rap2 (Fig. 8F, G), resulting in ~40-fold decrease in relative activity of Rap to Ras ($p<0.001$). Additionally, levels of phospho-ERK and GluA1, proteins downstream of Ras, were significantly higher in DN-Plk2 mice (Fig. 8H, I). However, phospho-p38 levels were unchanged, consistent

with DN-Plk2 expression in cultured neurons (Fig. S3F), suggesting the involvement of Rap-independent pathways in p38 activation. Thus, sustained disruption of Plk2 function hyperactivates Ras and impairs basal Rap signaling in mouse forebrain.

### Altered spine morphology in DN-Plk2 mice

DN-Plk2 brain exhibited no gross anatomical defects (Fig. S7B), although TG mice did exhibit slightly increased cortical thickness compared to WT animals (Fig. S7C–E). Golgi staining showed that pyramidal neurons in hippocampal area CA1, a region with robust DN-Plk2 expression (Fig. 8C, D), had significantly more and larger spines in proximal dendrites of DN-Plk2 mice, but no change in spine length (Fig. 8J–M; Table S1). The change in spine structure were confined to proximal dendritic regions with no differences in distal dendrites (Fig. S7F–I). Thus, disruption of Ras/Rap signaling by DN-Plk2 altered cortical structure and increased spine size and number *in vivo*.

### Aberrant memory formation in DN-Plk2 mice

To investigate whether dysregulation of Plk2 affected learning and memory, we tested spatial working memory on the T-maze (see Methods). Both WT and DN-Plk2 mice showed normal spontaneous alternation (~80%), an innate behavior dependent on the hippocampus (Lalonde, 2002), with similar latency to choose either arm, suggesting intact working memory and exploratory behavior of DN-Plk2 mice (Fig. 8N, O).

We next tested long-term spatial memory using the Morris water maze. Animals received four trials a day over six days, during which we observed no difference in latency to find the hidden platform between genotypes (Fig. 8P). However, in the probe trial conducted 48 h after the last training session, DN-Plk2 mice spent less time in the target quadrant compared to WT aniamls, at a level not significantly different from random chance (25% in each quadrant) (Fig. 8Q), indicating impairment of memory retention.

Finally, we performed fear conditioning, a type of long-term memory task that involves both hippocampus and amygdala. Mice were conditioned with two tone-shock pairings. Before training, baseline freezing was similar between genotypes (~2%) (Fig. 8R). Freezing was measured after 24 h in the same context in which training occurred. Interestingly, DN-Plk2 mice froze significantly *more* than WT animals (Fig. 8R) in this contextual paradigm. We also tested cued fear memory by exposing the mice to the tone in a novel context 48 h after training. Compared to low levels of pre-tone freezing in WT mice, TG mice showed markedly increased pre-tone freezing (Fig. 8S), suggesting DN-Plk2 mice had higher generalized fear levels after training irrespective of context. There was no difference in post-tone freezing between genotypes (Fig. 8S). Importantly, no significant difference was observed in shock sensitivity between genotypes (data not shown), excluding the possibility that the observed effects in DN-Plk2 mice were due to greater pain sensation. Together, these behavioral data indicate that disruption of Plk2 impairs proper memory formation as well as the setting of appropriate fear level.

## DISCUSSION

We have demonstrated that Plk2 coordinates the balance between Ras and Rap to downregulate synapses following chronic overactivity, and that this regulation is mediated by direct phosphorylation of an ensemble of Ras/Rap regulators—SPAR, RasGRF1, SynGAP, and PDZGEF1. We cannot rule out, however, the possibility that Plk2 may influence other GEFs/GAPs as well. Phosphorylation of SynGAP required the PBD of Plk2, which is also required for maximal efficiency of SPAR phosphorylation (Seeburg et al., 2008). Thus, in the brain the PBD appears to be a module that targets Plk2 preferentially to

substrates involved in control of Ras and Rap. Although not an exhaustive approach, the striking result that only Ras/Rap regulators were found to be positive phosphorylation substrates implicates Plk2 as a central component for controlling Ras and Rap signaling machinery.

### Inhibition of Ras and activation of Rap by Plk2

Plk2 is required for homeostatic downregulation of excitatory synaptic activity in hippocampal neurons in a SPAR and Cdk5-dependent manner (Seeburg et al., 2008). Based on the current work, we propose the following model for Plk2 function (Fig. S7J): synaptic activity induces expression of Plk2, which coordinately targets via PBD interactions to key regulators of Ras and Rap. Phosphorylation-dependent degradation of RasGRF1 (Ras activator), together with activation of SynGAP (Ras inhibitor), dramatically reduces active Ras levels. Conversely, degradation of SPAR (Rap inhibitor) and activation of PDZGEF1 (Rap activator) work additively to stimulate Rap. The result of this mirror-image regulatory program is a profound shift in favor of Rap at the expense of Ras. Indeed, quantification under various conditions of synaptic activity (or Plk2 function) revealed that Ras and Rap can be bidirectionally regulated by Plk2 over ~4000-fold difference in relative ratio of Rap to Ras activation state (Fig. S7K). Thus, we propose that Plk2 abundance may act as a graded sensor coupling synaptic activity level to the fine-tuning of Ras and Rap balance over a wide dynamic range.

### Plk2-directed spine remodeling via cooperative action of Ras/Rap regulators

In hippocampal neurons, silencing of Plk2 led to more and larger spines, consistent with a normal function for Plk2 in promoting spine shrinkage and loss (Pak and Sheng, 2003). These effects were also observed in hippocampus of DN-Plk2 mice. Importantly, PTX-mediated reduction of spine density and head width were abolished by blocking Plk2 activity using multiple independent methods. Therefore, Plk2 is required for homeostatic downregulation of dendritic spines in response to chronic overactivity.

Individual knockdown experiments as well as a series of epistasis tests demonstrated that each identified GAP/GEF acted downstream of Plk2 in controlling different aspects of dendritic spines. RasGRF1 consistently increased spine density, but also affected spine length and width in some assays. In contrast, PDZGEF1 selectively suppressed spine density. SynGAP reduced spine width, consistent with larger spines observed in SynGAP-deficient mice (Vazquez et al., 2004), while SPAR strongly increased head size along with exerting modest effects on spine density. These results suggest that, despite some overlap in function, each regulator fulfills a primary responsibility in homeostatic spine regulation, with RasGRF1 antagonistic to PDZGEF1 in controlling spine density, and SPAR opposing SynGAP in spine size control (Fig. S7L). These observations may explain the necessity of regulating both Ras and Rap signaling arms by Plk2. An alternative, but not mutually exclusive, possibility is that Plk2 actions on multiple GAPs/GEFs allow synergistic shifts in Ras and Rap balance.

### Plk2-directed phosphorylation of Ras/Rap regulators and functional implications

A detailed mechanistic examination of Plk2 phosphorylation sites on Ras/Rap regulators identified several novel phosphosites whose functional influence can be classified into three broad categories: 1) RasGRF1 phosphorylation sites were found in PH domains which suggests involvement in regulating subcellular distribution. We propose that PH domain phosphorylation by Plk2 leads to detachment from membranes, potentially increasing accessibility to proteasomal degradation. 2) Phosphorylation of both PDZGEF1 and SynGAP induced large gel mobility shifts suggestive of extensive conformational changes. Because these alterations were associated with increased enzymatic activity, we suggest

phosphorylation at these sites locks SynGAP or PDZGEF1 in an open, active conformation. 3) Additional phosphosites within or near the GAP domain of SynGAP (S326, S390) did not appear to be involved in conformational changes but did interfere with Plk2 ability to modulate SynGAP enzymatic activity, suggesting an independent mode of regulation that may involve direct GAP domain control.

Importantly, expression of Plk2 phosphorylation-deficient mutants of RasGRF1, SynGAP and PDZGEF1 abolished specific aspects of PTX-induced spine remodeling generally consistent with knockdown and overexpression studies, demonstrating that Plk2 phosphorylation of these Ras/Rap regulators is required for full homeostatic regulation of dendritic spines.

### Spatial and subunit-specific regulation of surface AMPARs

Overactivity-induced removal of sGluA1 was restricted to proximal dendrites and dependent on Plk2 kinase activity, mirroring RasGRF1/SPAR expression and dendritic spine loss. In contrast, hyperexcitation reduced sGluA2 in both proximal and distal dendrites through a Plk2 kinase-dependent and -independent mechanism, respectively. These results confirm and extend our previous findings that a kinase-independent interaction of Plk2 with NSF dislodges GluA2, causing loss of surface expression in secondary dendrites (Evers et al., 2010). Although it is currently unclear how these two mechanisms act on different dendritic subregions, these findings may suggest that GluA1 and GluA2 subserve distinct functions during homeostatic adaptation to overexcitation and support the idea that proximal dendrites employ a different or additional homeostatic mechanism from distal dendrites (Fig. S7J).

### A proximal dendritic homeostatic domain controlled by Plk2

Multiple mechanisms of homeostatic synaptic plasticity exist based on mode of activity manipulation, developmental stage, and cell type (Pozo and Goda, 2010). Here we elucidated two distinct and complementary mechanisms of homeostasis depending on dendritic locus as well as Plk2 kinase activity (Fig. S7J), with the following lines of evidence: Plk2 is induced in a proximal-to-distal gradient by chronic overactivity (Pak and Sheng, 2003). Plk2 kinase activity was required for depletion of RasGRF1/SPAR, PSD scaffold proteins, dendritic spines, as well as sGluA1/A2 specifically within the proximal dendrite. In contrast, PTX-induced sGluA2 removal in distal dendrites was kinase-independent. These results may reflect a need to regulate distal AMPARs via a graded, linear response in proportion to the level of synaptic activity experienced, but to control proximal dendritic synapses in an all-or-none fashion, potentially in response to more traumatic or persistent insults. Previous studies support the idea that homeostatic responses are spatially restricted. For example, CaMKIIβ mRNA is strikingly restricted to the soma and proximal dendrites (Martone et al., 1996) and its protein expression is dynamically regulated in homeostatic plasticity (Thiagarajan et al., 2002). AMPA-induced AMPAR internalization also occurs primarily in soma and proximal dendrites of hippocampal neurons (Biou et al., 2008). Together, these findings suggest a role of the proximal dendrite as a homeostatic domain and also emphasize the importance of specifying the dendritic subregion studied in homeostatic plasticity. This caveat may explain, at least in part, discrepancies in the literature regarding AMPAR subunits involved in homeostatic regulation.

### Essential *in vivo* requirement for Plk2 function in Ras/Rap regulation

The function of Plk2 *in vivo* has been explored previously using knockout animals, but not examined in synaptic plasticity (Inglis et al., 2009; Ma et al., 2003a). We used a dominant negative transgenic approach to address potential functional redundancy by binding to all shared targets of the Plk subfamily and inactivating them by sequestration. However, it is

highly likely that Plk2 is the relevant polo family kinase involved in activity-dependent homeostatic synaptic downregulation, based on the similar effect of Plk2 RNAi on spines in cultured neurons to DN-Plk2 expressed in TG animals, the absence of Plk1 and Plk4 expression in normal brain tissue (Winkles and Alberts, 2005), and lack of effect of Plk3 RNAi on PTX-induced homeostatic plasticity in any of our assays. The precise function of Plk3 in brain is unknown, but as this kinase was originally identified as an FGF-inducible factor, Plk3 may be responsive to neurotrophic or other growth factor stimulation.

DN-Plk2 animals exhibited increases in RasGRF1 and SPAR protein levels, similar to expression of DN-Plk2 in dissociated neuron culture. These effects were accompanied by elevated levels of active Ras and several phenotypes consistent with previously described consequences of Ras overactivity including increased ERK activation, slightly enlarged cortex (likely due to neuronal hypertrophy) (Heumann et al., 2000), higher spine density (Arendt et al., 2004), and elevated GluA1 expression (Kim et al., 2003). Perhaps the most striking observation was that TG forebrains had nearly undetectable levels of active Rap1 or Rap2. Thus, Plk2 appears to be critically required for Rap activation in the brain, at least under basal conditions of normal ongoing activity. It is nevertheless probable that Plk2-independent pathways to Ras and Rap regulation exist, particularly under conditions of acute plasticity or stimulation (Woolfrey et al., 2009).

### Physiological roles of Plk2 *in vivo*

Ras signaling plays critical roles in learning and memory (Mazzucchelli and Brambilla, 2000). Somewhat surprisingly, DN-Plk2 mice exhibited normal working memory and no deficit in acquisition of the Morris water maze task. However, TG mice showed slightly impaired memory retention when subjected to probe tests. Ras/Rap activity (or more likely, the balance between the two) may play direct roles in memory mechanisms, as H-Ras knockout mice exhibit enhanced LTP (Manabe et al., 2000), and Rap1N17 (dominant negative) expressing mice demonstrate deficient LTP (Morozov et al., 2003). Alternatively, homeostatic function may be permissive for effective expression of Hebbian plasticity, as inactivation of Plk2 causes run-up of synaptic transmission in hippocampal slices that prevents induction of subsequent LTP (Seeburg and Sheng, 2008).

A more pronounced behavioral outcome was uncovered during cued fear conditioning, which revealed that DN-Plk2 mice experienced similar basal fear compared to WT animals, but failed to restrain their fear levels after tone-shock pairing. This result could explain the apparently enhanced freezing behavior in the contextual fear conditioning. Together, our behavioral results indicate that imbalance of Ras and Rap by Plk2 interference is detrimental for stabilization of memory and setting of fear levels within an appropriate range.

It is worth noting that the Plk2 kinase-independent pathway could explain some of the phenotypes of the DN-Plk2 TG mouse, which is impaired for the kinase-dependent pathway but not the effects of Plk2 on NSF. Thus, the DN-Plk2 mice would be expected to exhibit a mixed phenotype: loss of some sGluA2 and synapse weakening through the kinase-independent mechanism, together with a gain of dendritic spines and increased Ras signaling due to impaired Plk2 kinase-dependent pathways. In general, however, the biochemical, morphological, and behavioral phenotypes reported (more and larger spines, enlarged cortex, increased RasGRF1 and SPAR levels, increased Ras activity, and elevated fear) were not consistent with loss of functional GluA2, but rather are better explained by interference with Plk2 kinase function. These phenotypes suggest the kinase-dependent pathway may be the dominant mechanism in these mice. However, the unexpectedly minor deficits in the water maze test and the lack of seizure sensitivity (data not shown) in these animals suggest that weakening of synapses with GluA2 removal may have partially compensated for the run-up in excitatory synapse size and number due to loss of Plk2 negative homeostatic

function, leading to potentially less severe hyperactivity and learning phenotypes than with complete loss of Plk2 expression.

Although we proposed that Plk2 operates over a wide spectrum of activity levels, it seems plausible that its dampening influence would be most critically needed during episodes of extreme overactivity. Thus, homeostatic restraint of heightened synaptic activity following the strongest forms of environmental stimuli may represent scenarios in which Plk2-mediated control of Ras and Rap in proximal dendrites is most relevant and valuable for animal behavior.

## Experimental Procedures

### Plk2 kinase assay

GST-tagged Plk2 mutants (KD or CA) expressed in COS-7 cells were coupled to glutathione-Sepharose beads (Amersham Biosciences) and washed in kinase buffer (50 mM Tris pH 7.5, 10 mM $MgCl_2$, 5 mM DTT, 2 mM EGTA and 2 μM microcystin LR). Candidate substrates expressed in COS-7 cells were immunoprecipitated and incubated with either KD or CA Plk2 in the presence of 50 μM ATP and 10 μCi of $^{32}$P-γ-ATP (6000 Ci/mmol, Amersham) for 30 min at 30°C with continuous agitation in a Thermomixer (Eppendorf). Samples were subjected to SDS-PAGE and gels dried for autoradiography.

### Active Ras and Rap pulldown assay

Transfected COS-7 cells or cultured hippocampal neurons were harvested in lysis buffer (25 mM Tris-HCl pH 7.4, 250 mM NaCl, 0.5% NP40, 1.25 mM $MgCl_2$ and 5% glycerol). Cell lysates or mouse brain homogenates were centrifuged, and supernatants were incubated with 20 μl of GST-Raf1-RBD or GST-RalGDS-RBD coupled to glutathione sepharose (Amersham) for 3 h at 4ºC. Pellets were washed three times in 0.5 ml lysis buffer and analyzed by western blotting.

Additional detailed methods can be found in online Supplementary Information.

## Supplementary Material

Refer to Web version on PubMed Central for supplementary material.

## Acknowledgments

We thank Josefina Lam for technical assistance. This study was supported by NIH grant NS048085 (DTSP).

## References

Arendt T, Gartner U, Seeger G, Barmashenko G, Palm K, Mittmann T, Yan L, Hummeke M, Behrbohm J, Bruckner MK, et al. Neuronal activation of Ras regulates synaptic connectivity. Eur J Neurosci. 2004; 19:2953–2966. [PubMed: 15182302]

Biou V, Bhattacharyya S, Malenka RC. Endocytosis and recycling of AMPA receptors lacking GluR2/3. Proc Natl Acad Sci U S A. 2008; 105:1038–1043. [PubMed: 18195348]

Brambilla R, Gnesutta N, Minichiello L, White G, Roylance AJ, Herron CE, Ramsey M, Wolfer DP, Cestari V, Rossi-Arnaud C, et al. A role for the Ras signalling pathway in synaptic transmission and long-term memory. Nature. 1997; 390:281–286. [PubMed: 9384379]

Buchsbaum R, Telliez JB, Goonesekera S, Feig LA. The N-terminal pleckstrin, coiled-coil, and IQ domains of the exchange factor Ras-GRF act cooperatively to facilitate activation by calcium. Mol Cell Biol. 1996; 16:4888–4896. [PubMed: 8756648]

Chen HJ, Rojas-Soto M, Oguni A, Kennedy MB. A synaptic Ras-GTPase activating protein (p135 SynGAP) inhibited by CaM kinase II. Neuron. 1998; 20:895–904. [PubMed: 9620694]

de Rooij J, Boenink NM, van Triest M, Cool RH, Wittinghofer A, Bos JL. PDZ-GEF1, a guanine nucleotide exchange factor specific for Rap1 and Rap2. J Biol Chem. 1999; 274:38125–38130. [PubMed: 10608883]

de Rooij J, Bos JL. Minimal Ras-binding domain of Raf1 can be used as an activation-specific probe for Ras. Oncogene. 1997; 14:623–625. [PubMed: 9053862]

Evers DM, Matta JA, Hoe HS, Zarkowsky D, Lee SH, Isaac JT, Pak DT. Plk2 attachment to NSF induces homeostatic removal of GluA2 during chronic overexcitation. Nat Neurosci. 2010; 13:1199–1207. [PubMed: 20802490]

Fu Z, Lee SH, Simonetta A, Hansen J, Sheng M, Pak DT. Differential roles of Rap1 and Rap2 small GTPases in neurite retraction and synapse elimination in hippocampal spiny neurons. J Neurochem. 2007; 100:118–131. [PubMed: 17227435]

Heumann R, Goemans C, Bartsch D, Lingenhohl K, Waldmeier PC, Hengerer B, Allegrini PR, Schellander K, Wagner EF, Arendt T, et al. Transgenic activation of Ras in neurons promotes hypertrophy and protects from lesion-induced degeneration. J Cell Biol. 2000; 151:1537–1548. [PubMed: 11134081]

Inglis KJ, Chereau D, Brigham EF, Chiou SS, Schobel S, Frigon NL, Yu M, Caccavello RJ, Nelson S, Motter R, et al. Polo-like kinase 2 (PLK2) phosphorylates alpha-synuclein at serine 129 in central nervous system. J Biol Chem. 2009; 284:2598–2602. [PubMed: 19004816]

Kauselmann G, Weiler M, Wulff P, Jessberger S, Konietzko U, Scafidi J, Staubli U, Bereiter-Hahn J, Strebhardt K, Kuhl D. The polo-like protein kinases Fnk and Snk associate with a Ca(2+)- and integrin-binding protein and are regulated dynamically with synaptic plasticity. Embo J. 1999; 18:5528–5539. [PubMed: 10523297]

Kim JH, Lee HK, Takamiya K, Huganir RL. The role of synaptic GTPase-activating protein in neuronal development and synaptic plasticity. J Neurosci. 2003; 23:1119–1124. [PubMed: 12598599]

Kim JH, Liao D, Lau LF, Huganir RL. SynGAP: a synaptic RasGAP that associates with the PSD-95/SAP90 protein family. Neuron. 1998; 20:683–691. [PubMed: 9581761]

Komiyama NH, Watabe AM, Carlisle HJ, Porter K, Charlesworth P, Monti J, Strathdee DJ, O'Carroll CM, Martin SJ, Morris RG, et al. SynGAP regulates ERK/MAPK signaling, synaptic plasticity, and learning in the complex with postsynaptic density 95 and NMDA receptor. J Neurosci. 2002; 22:9721–9732. [PubMed: 12427827]

Krapivinsky G, Krapivinsky L, Manasian Y, Ivanov A, Tyzio R, Pellegrino C, Ben-Ari Y, Clapham DE, Medina I. The NMDA receptor is coupled to the ERK pathway by a direct interaction between NR2B and RasGRF1. Neuron. 2003; 40:775–784. [PubMed: 14622581]

Lalonde R. The neurobiological basis of spontaneous alternation. Neurosci Biobehav Rev. 2002; 26:91–104. [PubMed: 11835987]

Lee KS, Grenfell TZ, Yarm FR, Erikson RL. Mutation of the polo-box disrupts localization and mitotic functions of the mammalian polo kinase Plk. Proc Natl Acad Sci U S A. 1998; 95:9301–9306. [PubMed: 9689075]

Lenart P, Petronczki M, Steegmaier M, Di Fiore B, Lipp JJ, Hoffmann M, Rettig WJ, Kraut N, Peters JM. The small-molecule inhibitor BI 2536 reveals novel insights into mitotic roles of polo-like kinase 1. Curr Biol. 2007; 17:304–315. [PubMed: 17291761]

Liao Y, Kariya K, Hu CD, Shibatohge M, Goshima M, Okada T, Watari Y, Gao X, Jin TG, Yamawaki-Kataoka Y, Kataoka T. RA-GEF, a novel Rap1A guanine nucleotide exchange factor containing a Ras/Rap1A-associating domain, is conserved between nematode and humans. J Biol Chem. 1999; 274:37815–37820. [PubMed: 10608844]

Ma S, Charron J, Erikson RL. Role of Plk2 (Snk) in mouse development and cell proliferation. Mol Cell Biol. 2003a; 23:6936–6943. [PubMed: 12972611]

Ma S, Liu MA, Yuan YL, Erikson RL. The serum-inducible protein kinase Snk is a G1 phase polo-like kinase that is inhibited by the calcium- and integrin-binding protein CIB. Mol Cancer Res. 2003b; 1:376–384. [PubMed: 12651910]

Manabe T, Aiba A, Yamada A, Ichise T, Sakagami H, Kondo H, Katsuki M. Regulation of long-term potentiation by H-Ras through NMDA receptor phosphorylation. J Neurosci. 2000; 20:2504–2511. [PubMed: 10729330]

Martone ME, Pollock JA, Jones YZ, Ellisman MH. Ultrastructural localization of dendritic messenger RNA in adult rat hippocampus. J Neurosci. 1996; 16:7437–7446. [PubMed: 8922399]

Mayford M, Bach ME, Huang YY, Wang L, Hawkins RD, Kandel ER. Control of memory formation through regulated expression of a CaMKII transgene. Science. 1996; 274:1678–1683. [PubMed: 8939850]

Mazzucchelli C, Brambilla R. Ras-related and MAPK signalling in neuronal plasticity and memory formation. Cell Mol Life Sci. 2000; 57:604–611. [PubMed: 11130460]

Morozov A, Muzzio IA, Bourtchouladze R, Van-Strien N, Lapidus K, Yin D, Winder DG, Adams JP, Sweatt JD, Kandel ER. Rap1 couples cAMP signaling to a distinct pool of p42/44MAPK regulating excitability, synaptic plasticity, learning, and memory. Neuron. 2003; 39:309–325. [PubMed: 12873387]

Ohtsuka T, Hata Y, Ide N, Yasuda T, Inoue E, Inoue T, Mizoguchi A, Takai Y. nRap GEP: a novel neural GDP/GTP exchange protein for rap1 small G protein that interacts with synaptic scaffolding molecule (S-SCAM). Biochem Biophys Res Commun. 1999; 265:38–44. [PubMed: 10548487]

Pak DT, Sheng M. Targeted protein degradation and synapse remodeling by an inducible protein kinase. Science. 2003; 302:1368–1373. [PubMed: 14576440]

Pak DT, Yang S, Rudolph-Correia S, Kim E, Sheng M. Regulation of dendritic spine morphology by SPAR, a PSD-95-associated RapGAP. Neuron. 2001; 31:289–303. [PubMed: 11502259]

Pozo K, Goda Y. Unraveling mechanisms of homeostatic synaptic plasticity. Neuron. 2010; 66:337–351. [PubMed: 20471348]

Ryu J, Futai K, Feliu M, Weinberg R, Sheng M. Constitutively active Rap2 transgenic mice display fewer dendritic spines, reduced extracellular signal-regulated kinase signaling, enhanced long-term depression, and impaired spatial learning and fear extinction. J Neurosci. 2008; 28:8178–8188. [PubMed: 18701680]

Seeburg DP, Feliu-Mojer M, Gaiottino J, Pak DT, Sheng M. Critical role of CDK5 and Polo-like kinase 2 in homeostatic synaptic plasticity during elevated activity. Neuron. 2008; 58:571–583. [PubMed: 18498738]

Seeburg DP, Sheng M. Activity-induced Polo-like kinase 2 is required for homeostatic plasticity of hippocampal neurons during epileptiform activity. J Neurosci. 2008; 28:6583–6591. [PubMed: 18579731]

Shepherd JD, Huganir RL. The cell biology of synaptic plasticity: AMPA receptor trafficking. Annu Rev Cell Dev Biol. 2007; 23:613–643. [PubMed: 17506699]

Thiagarajan TC, Piedras-Renteria ES, Tsien RW. alpha- and betaCaMKII. Inverse regulation by neuronal activity and opposing effects on synaptic strength. Neuron. 2002; 36:1103–1114. [PubMed: 12495625]

Turrigiano GG. The self-tuning neuron: synaptic scaling of excitatory synapses. Cell. 2008; 135:422–435. [PubMed: 18984155]

Vazquez LE, Chen HJ, Sokolova I, Knuesel I, Kennedy MB. SynGAP regulates spine formation. J Neurosci. 2004; 24:8862–8872. [PubMed: 15470153]

Winkles JA, Alberts GF. Differential regulation of polo-like kinase 1, 2, 3, and 4 gene expression in mammalian cells and tissues. Oncogene. 2005; 24:260–266. [PubMed: 15640841]

Woolfrey KM, Srivastava DP, Photowala H, Yamashita M, Barbolina MV, Cahill ME, Xie Z, Jones KA, Quilliam LA, Prakriya M, Penzes P. Epac2 induces synapse remodeling and depression and its disease-associated forms alter spines. Nat Neurosci. 2009; 12:1275–1284. [PubMed: 19734897]

Wu GY, Deisseroth K, Tsien RW. Spaced stimuli stabilize MAPK pathway activation and its effects on dendritic morphology. Nat Neurosci. 2001; 4:151–158. [PubMed: 11175875]

Ye X, Carew TJ. Small G protein signaling in neuronal plasticity and memory formation: the specific role of ras family proteins. Neuron. 2010; 68:340–361. [PubMed: 21040840]

Zhu JJ, Qin Y, Zhao M, Van Aelst L, Malinow R. Ras and Rap control AMPA receptor trafficking during synaptic plasticity. Cell. 2002; 110:443–455. [PubMed: 12202034]

Zhu Y, Pak D, Qin Y, McCormack SG, Kim MJ, Baumgart JP, Velamoor V, Auberson YP, Osten P, van Aelst L, et al. Rap2-JNK removes synaptic AMPA receptors during depotentiation. Neuron. 2005; 46:905–916. [PubMed: 15953419]

Zwartkruis FJ, Wolthuis RM, Nabben NM, Franke B, Bos JL. Extracellular signal-regulated activation of Rap1 fails to interfere in Ras effector signalling. Embo J. 1998; 17:5905–5912. [PubMed: 9774335]

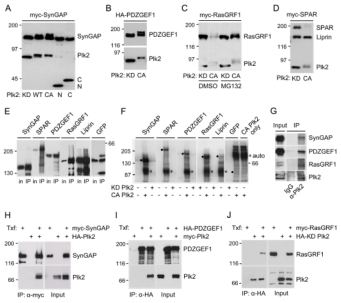


**Figure 1. Plk2 interacts with and phosphorylates Ras and Rap GEFs/GAPs**

**(A)** Gel mobility shift of SynGAP induced by cotransfected wild-type (WT) or constitutively active (CA) Plk2 in COS-7 cells, but not by kinase-dead (KD) Plk2 or Plk2 N/C-terminal fragments. **(B)** Gel mobility shift of PDZGEF1 by cotransfected CA Plk2 but not KD Plk2. **(C)** RasGRF1 was cotransfected with KD or CA Plk2 in COS-7 cells, treated with MG132 (25 μM, 16 h) or vehicle (DMSO), and lysates immunoblotted as shown at right of blots. **(D)** COS-7 cells were transfected with SPAR and KD or CA Plk2. Cotransfected liprin was used as internal negative control and transfection/loading control. **(E)** Proteins as indicated at top were immunoprecipitated 24 h after transfection and recovery examined by immunoblotting. In, input; IP, immunoprecipitation. **(F)** Immunoprecipitates from (E) were incubated with $^{32}$P-γ-ATP and purified KD or CA Plk2 (except in last lane, containing CA Plk2 only). Black dots indicate expected sizes of indicated proteins. Autophosphorylated CA Plk2 (auto) was marked with asterisks. Liprin and GFP were used as negative controls. Note right-most panel was run on higher percentage gel to resolve GFP. **(G)** Mouse brain lysates (Input) were immunoprecipitated with rabbit anti-Plk2 antibody (7382) or IgG control and immunoblotted for Ras/Rap regulators as indicated. **(H–J)** COS-7 cells were transfected as indicated at top of blots, with IP performed as shown at bottom and western blotting for transfected proteins as indicated at right of each blot. KD Plk2 was used in (J) to prevent loss of RasGRF1 by active Plk2. Input, 10% of lysate used for each IP. All MW in kDa.

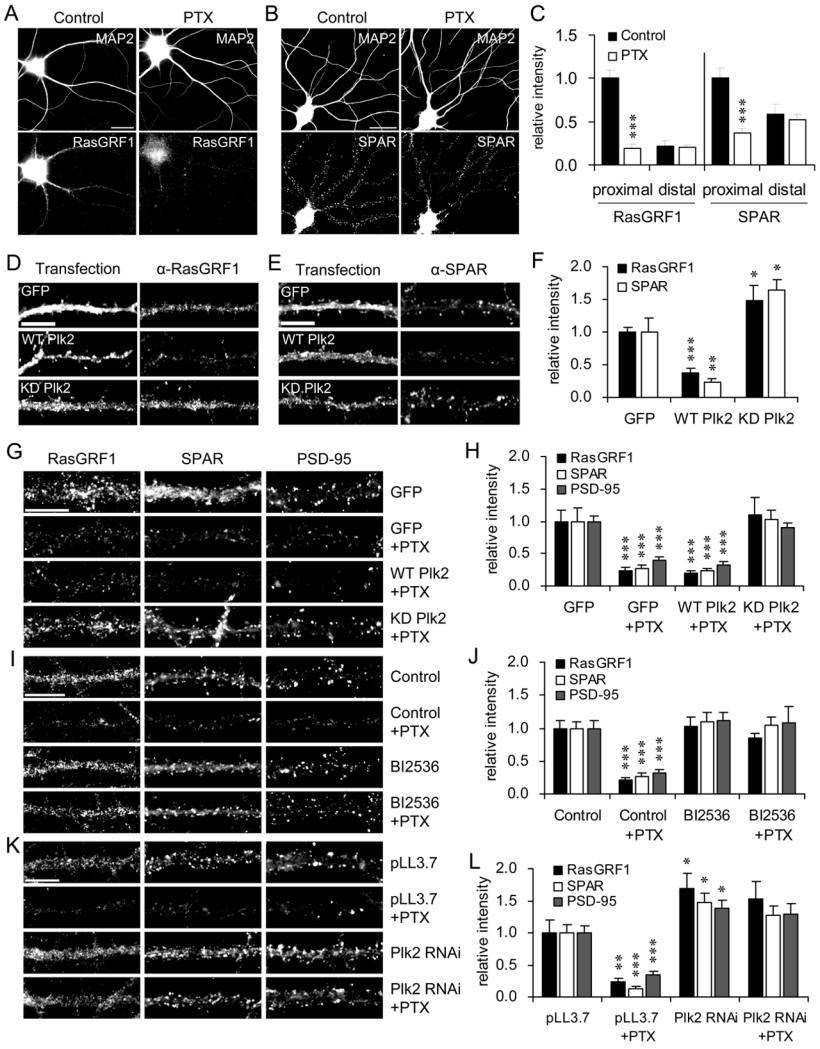


**Figure 2. Plk2 induced by overactivity eliminates RasGRF1 and SPAR in neurons**

**(A–B)** Cultured hippocampal neurons (20–23 DIV) were treated with PTX (100 μM, 20 h) or vehicle and immunolabeled for RasGRF1 and SPAR. MAP2 staining is shown to outline dendrites. Scale, 20 μm. **(C)** Quantification of integrated intensity of RasGRF1 and SPAR (n=10). **(D and E)** Neurons were transfected with pEGFP, WT Plk2, or KD Plk2 for 3 days followed by immunostaining for RasGRF1 and SPAR. Scale, 10 μm. **(F)** Quantification of integrated intensity of RasGRF1 and SPAR in proximal dendrites (n=10). **(G)** Hippocampal cultures were infected with Sindbis virus expressing GFP, WT Plk2 or KD Plk2, treated with PTX, then immunostained for RasGRF1, SPAR, and PSD-95. Scale, 10 μm. **(H)** Quantification of integrated intensity from (G) in proximal dendrites (n=10–11). **(I)** Neurons were treated with PTX in the presence of Plk inhibitor BI2536 (75 nM, 20 h) or vehicle as indicated, and then immunostained for RasGRF1, SPAR, and PSD-95. Scale, 10 μm. **(J)** Quantification of integrated intensity from (I) in proximal dendrites (n=10). **(K)** Hippocampal neurons were transfected with Plk2-shRNA or control (pLL3.7) vector. After 48 h, cells were treated with PTX or vehicle and immunolabeled for RasGRF1, SPAR and PSD-95. Scale, 10 μm. **(L)** Quantification of integrated intensity from (K) (n=10). *p<0.05, **p<0.01, ***p<0.001 for all graphs.

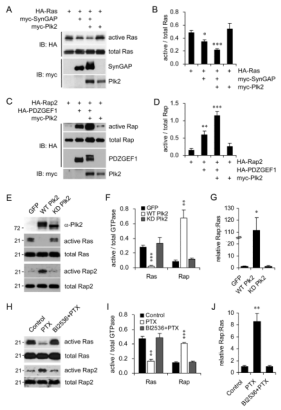

**Figure 3. Plk2 stimulates SynGAP and PDZGEF1 to regulate Ras and Rap**

**(A)** COS-7 cells were transfected as indicated at top of blot. Cell lysates were incubated with GST-Raf1-RBD to precipitate active Ras, followed by immunoblotting (IB) as indicated. **(B)** Quantification of active Ras normalized to total Ras (n=6). **(C)** Lysates of COS-7 cells transfected as indicated at top were incubated with GST-RalGDS-RBD to precipitate active Rap, followed by IB analysis. **(D)** Quantification of active Rap2 normalized to total Rap2 (n=6). **(E)** Active Ras and Rap pulldown assays in cultured hippocampal neurons. Cells (19–21 DIV) were infected with Sindbis virus expressing GFP, WT Plk2, or KD Plk2. GST-Raf1-RBD and GST-RalGDS-RBD were used to pull down active Ras and Rap, respectively. **(F)** Quantification of active H-Ras and Rap2 normalized to total expression (n=5 and 7, respectively). **(G)** Relative fold change in Rap vs Ras activity. **(H)** Hippocampal neurons were stimulated with PTX in the presence or absence of BI2536. Active Ras and Rap pulldown assays were performed with GST-Raf1-RBD and GST-RalGDS-RBD. **(I)** Quantification of active H-Ras and Rap2 normalized to total expression (n=3–4). **(J)** Relative fold change in Rap vs Ras activity. *p<0.05, **p<0.01, ***p<0.001 for all graphs.

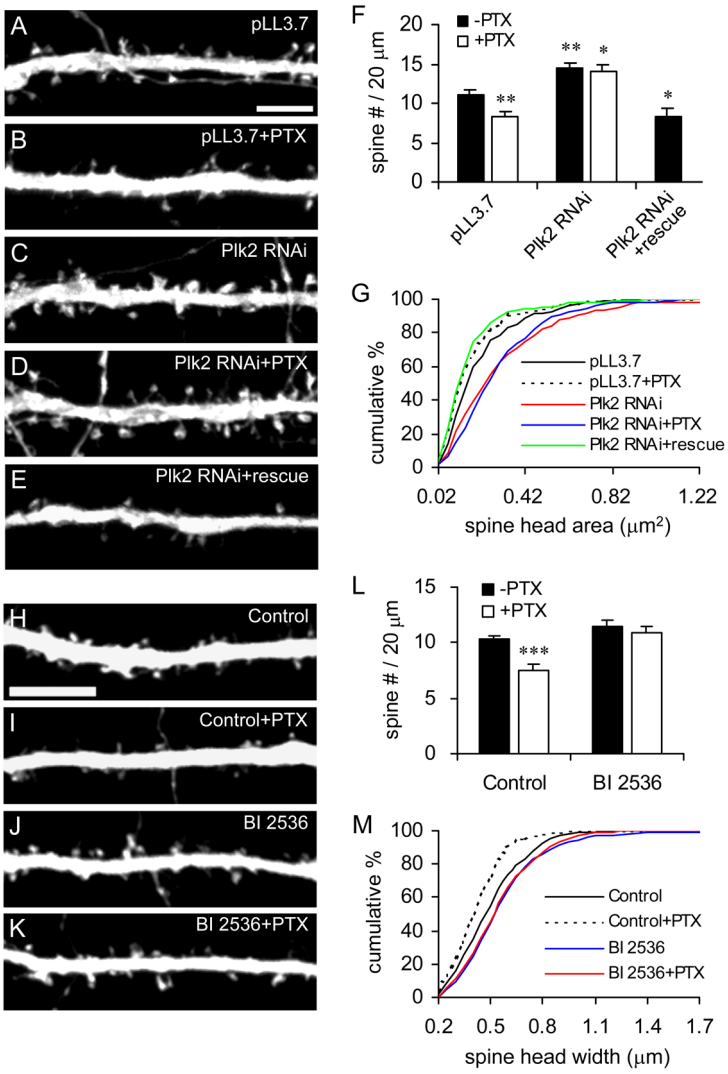


**Figure 4. Requirement for Plk2 in chronic overactivity-dependent spine remodeling**

**(A–E)** Cultured hippocampal neurons (21 DIV) were transfected with control vector (pLL3.7) containing CMV-EGFP, Plk2-shRNA, or Plk2-shRNA plus rescue construct. After 48 h, cells were treated with PTX or vehicle, and immunolabeled against GFP. Scale, 5 µm. **(F)** Quantification of spine density (n=10–11, *p<0.05, **p<0.01). **(G)** Cumulative frequency plot of spine head area (n=262–357 spines; Kolmogorov–Smirnov (K–S) test; Table S1). **(H–K)** Neurons were transfected with EGFP plasmid. After 48 h, cells were treated with or without PTX in the presence of BI2536 or vehicle, and then immunostained for GFP. Scale, 5 µm. **(L)** Quantification of spine density (n=12, ***p<0.001). **(M)** Cumulative frequency plot of spine head width (n=200 spines; K–S test; Table S1).

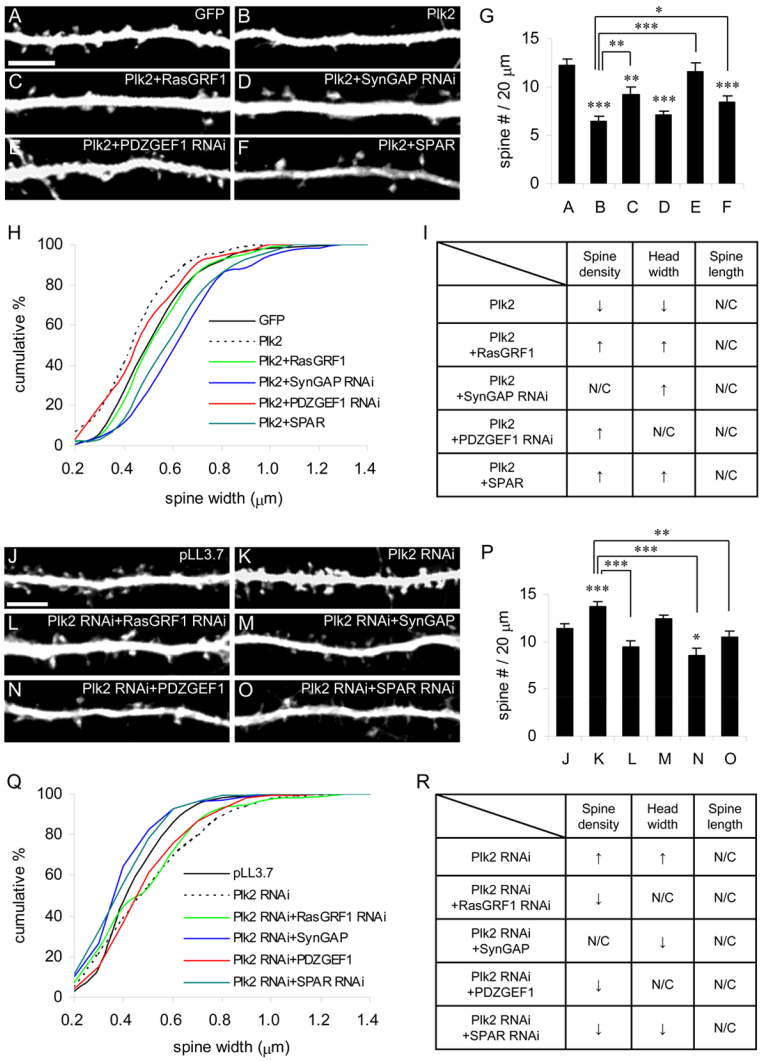


| | Spine density | Head width | Spine length |
|---|---|---|---|
| Plk2 | ↓ | ↓ | N/C |
| Plk2 +RasGRF1 | ↑ | ↑ | N/C |
| Plk2 +SynGAP RNAi | N/C | ↑ | N/C |
| Plk2 +PDZGEF1 RNAi | ↑ | N/C | N/C |
| Plk2 +SPAR | ↑ | ↑ | N/C |

| | Spine density | Head width | Spine length |
|---|---|---|---|
| Plk2 RNAi | ↑ | ↑ | N/C |
| Plk2 RNAi +RasGRF1 RNAi | ↓ | N/C | N/C |
| Plk2 RNAi +SynGAP | N/C | ↓ | N/C |
| Plk2 RNAi +PDZGEF1 | ↓ | N/C | N/C |
| Plk2 RNAi +SPAR RNAi | ↓ | ↓ | N/C |

**Figure 5. Plk2-induced spine remodeling is mediated by Ras- and Rap-GEFs/GAPs**

**(A–F)** Hippocampal neurons (21 DIV) were transfected as indicated, along with pEGFP to visualize spine morphology. After 3 days, cells were immunostained for GFP. Scale, 5 μm. **(G)** Quantification of spine density from (A–F) (n=10–11, *p<0.05, **p<0.01, ***p<0.001). **(H)** Cumulative frequency plot of spine head area (n=150–200 spines; K–S test; Table S1). **(I)** Summary of spine remodeling. Plk2 was compared to GFP control, while other conditions were compared to Plk2. **(J–O)** Cultured neurons were transfected as indicated for 3 days, followed by immunocytochemistry for GFP. Scale, 5 μm. **(P)** Quantification of spine density from (J–O) (n=10–11, *p<0.05, **p<0.01, ***p<0.001). **(Q)** Cumulative frequency plot of spine head area (n=150–250 spines; K–S test; Table S1). **(R)** Summary of spine remodeling. Plk2 RNAi was compared to control vector (pLL3.7), while other conditions were compared to Plk2 RNAi.

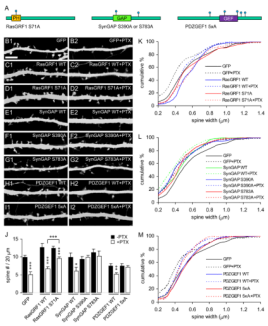

**Figure 6. Phosphomutation of Ras/Rap regulators prevents overactivity-dependent spine remodeling**

**(A)** Schematic of phosphomutants used: RasGRF1 (S71A), SynGAP (S390A or S783A), and quintuple PDZGEF1 mutant (5×A). **(B–I)** Hippocampal neurons (DIV19) were transfected with pEGFP and either WT or phosphomutant constructs. After 48 h, neurons were treated with PTX or vehicle, followed by immunostaining for GFP. Scale, 5 μm. **(J)** Quantification of spine density from (B–I) (n=8–11, *p<0.05, **p<0.01, ***p<0.001). **(K–M)** Cumulative frequency plot of spine head width (n=150–200 spines; K–S test; Table S1).

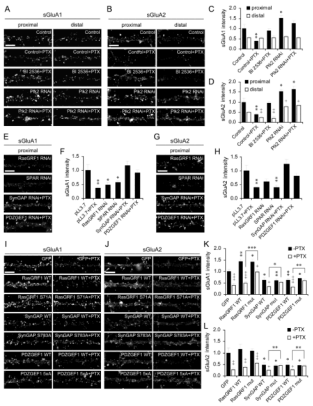

**Figure 7. Plk2 phosphorylation of Ras/Rap regulators is required for overactivity-induced downregulation of surface AMPARs**

**(A, B)** Hippocampal neurons (DIV19) were transfected with Plk2-shRNA or control vector (pLL3.7) and treated with or without PTX in the presence of BI2536 or vehicle. Immunostaining is shown for surface GluA1 or GluA2 in proximal and distal dendrites as indicated. Scale, 5 μm. **(C, D)** Quantification of integrated intensity for surface GluA1 (C) and GluA2 (D) (n=10–15, *p<0.05, **p<0.01 vs. proximal control; $^{+}$p<0.05, $^{++}$p<0.01 vs. distal control). **(E, G)** Neurons were transfected as indicated, treated with PTX or vehicle, and immunolabeled for surface GluA1 and GluA2. Scale, 5 μm. **(F, H)** Quantification of integrated intensity for surface GluA1 (F) and GluA2 (H) (n=10–15, *p<0.05, **p<0.01). **(I, J)** Neurons were transfected with pEGFP and either wild-type or phosphomutant constructs. After 48 h, neurons were treated with PTX or vehicle, followed by immunostaining for surface GluA1 and GluA2. Scale, 5 μm. **(K, L)** Quantification of integrated intensity for surface GluA1 (K) and GluA2 (L) (n=10–15, *p<0.05, **p<0.01, ***p<0.001 vs. GFP; $^{+}$p<0.05, $^{++}$p<0.01, $^{+++}$p<0.001 vs. -PTX).

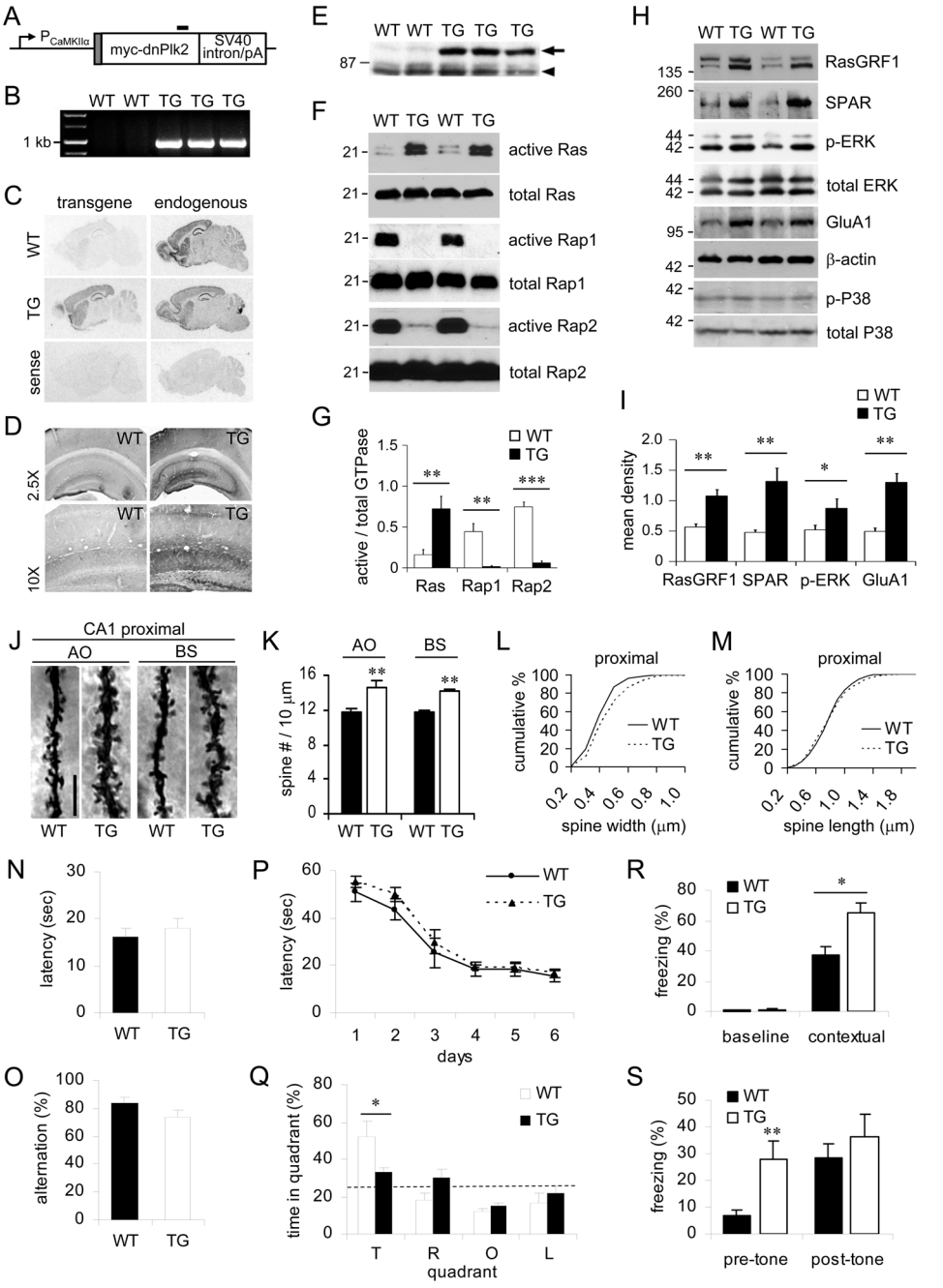


**Figure 8. Altered Ras and Rap signaling, spine morphogenesis and impaired memory in DN-Plk2 mice**

**(A)** Schematic representation of DN-Plk2 transgene (TG) construct. Gray bar, myc-epitope tag. Black bar, TG-specific in situ hybridization probe. **(B)** PCR genotyping of TG mice. **(C)** In situ hybridization of mRNA for transgenic and endogenous Plk2. **(D)** Immunohistochemistry of TG and WT brain sections (higher magnification images shown at bottom). **(E)** Western blot analysis of forebrain extracts. Transgene band (arrow) is larger than endogenous Plk2 (arrowhead) due to additional myc epitope. **(F)** Pulldown of active Ras, Rap1, and Rap2 in brain lysates from WT and DN-Plk2 mice using GST-Raf1-RBD and GST-RalGDS-RBD. **(G)** Quantification of active Ras, Rap1 and Rap2 normalized to

total expression (n=5, **p<0.01, ***p<0.001). **(H)** Immunoblotting of forebrain lysates from WT and DN-Plk2 mice against proteins indicated at right of blots. **(I)** Quantification of data from (H) normalized to β-actin or total ERK (n=5–10, *p<0.05, **p<0.01). **(J)** Proximal dendritic segments from hippocampal CA1 pyramidal neurons. Spines were quantified separately on apical oblique (AO) and basal (BS) dendrites. Scale, 5 μm. **(K–M)** Quantification of spine density (K), head width (L), and length (M) (n=6, **p<0.01; head width, K–S test, p<0.001). **(N, O)** Spontaneous alternation of WT and DN-Plk2 mice (n=6) in the T-maze, quantified by latency to select an arm (N) and percent alternation (O). **(P, Q)** Morris water maze test (n=6). Latency to find the platform (P) was recorded as index of learning, and probe test (Q) was performed 2 days after training (*p<0.05). Dashed line indicates chance level of quadrant exploration time. T, target; R, right, O, opposite, and L, left of target. **(R, S)** Fear conditioning. Mice were conditioned with two tone-shock pairing, then tested for contextual fear (R) at 24 h and cued fear (S) at 48 h (WT, n=10; TG, n=7; **p<0.01).